Baku State University: Journal of Physics & Space Sciences, **2026**, v3 (2), pp. 78-84

journal homepage: http://bsuj.bsu.edu.az/en

Dielectric Properties of Magnetite-Containing Core–Satellite-Type Structures

[1]Habiba A. Shirinova*, [1]Maarif A. Jafarov, [2]Bakhtiyar G. Pashayev, [3]Shirkhan A. Humbatov, [1]Shovkat Z. Najafzada

[1]Department of Chemical physics of nanomaterials, Baku State University, Baku, Azerbaijan;
[2]Department of Optics and molecular physics, Baku State University, Baku, Azerbaijan;
[3]Department of Physical Electronics, Baku State University, Baku, Azerbaijan.

Received 24-Apr.-2026; Accepted 05-Jun.-2026
DOI: https://doi.org/10.30546/209501.101.2026.3.02.643

Abstract

$BaTiO_3$–Fe_3O_4 core–satellite particles were synthesized and incorporated into a PVDF matrix to obtain hybrid nanocomposite films. XRD analysis revealed reflections at 31.53°, 35.59°, 56.12°, and 62.73°, confirming the coexistence of tetragonal $BaTiO_3$ and cubic Fe_3O_4 phases in the hybrid structure. Dielectric spectroscopy in the range 25 Hz to 1 MHz showed a frequency-dependent decrease in dielectric permittivity for all compositions, consistent with the reduced contribution of interfacial polarization at higher frequencies. The dielectric constant of neat PVDF was about 8 at 1 kHz, while the addition of hybrid filler increased this value. For the sample containing 7% $BaTiO_3$–Fe_3O_4, the dielectric permittivity reached values close to 60. These findings confirm that the introduction of $BaTiO_3$–Fe_3O_4 hybrid particles substantially enhances the polarization capability of the polymer matrix and improves the dielectric characteristics of the resulting nanocomposites

Keywords: Nanocomposite, magnetite, dielectric propertied, dielectric polarization
PACS Numbers: 75.50.−y, 61.46.+w, 61.46.−w, 51.70.+f

1. Introduction

In recent decades, the intensive development of nanotechnology has led to the creation of a new class of functional materials, namely nanocomposites with con-

*Corresponding author – Tel.: (+994) 70 208 03 06
e-mail address: habiba.shirinova@bsu.edu.az; *ORCID ID*: 0000-0003-3227-7752.

trollable structure and properties[1]. Of particular interest are magnetic nanostructures based on iron oxides, especially Fe_3O_4, due to their unique combination of magnetic, catalytic, and electrochemical characteristics[2-3]. Such materials have found wide application in catalysis, biomedicine, sensing, energy, and environmental technologies [4].

One of the most promising directions is the development of nanocomposites with core–shell and core–satellite architectures, which make it possible to purposefully combine the properties of different components within a single system[5-8]. In core–shell structures, the inner core provides the basic functional properties, such as magnetic or conductive behavior, while the shell performs a protective, stabilizing, or functionalizing role [9]. In turn, core–satellite structures are characterized by the presence of nanoparticles distributed over the surface of a magnetic core, which increases the active surface area and enhances interfacial interactions [10].

Such hybrid structures exhibit a pronounced synergistic effect [11]. For example, the presence of metallic nanoparticles promotes faster electron transfer and higher catalytic activity, while the magnetic core enables efficient separation of the material from the reaction medium by means of an external magnetic field. The relevance of research in this field is also determined by the need to address environmental and energy-related challenges. In particular, the development of efficient nanocatalysts makes it possible to reduce toxic organic compounds into less hazardous products and to create highly sensitive sensor systems for detecting environmental pollutants. Thus, the development and study of Fe_3O_4-based nanocomposites with controlled core–shell and core–satellite morphology represent an important scientific task. Investigation of their structure, properties, and interaction mechanisms opens broad prospects for the creation of new functional materials with tailored characteristics for application in various fields of science and technology.

The aim of this work is to synthesize $BaTiO_3$-Fe_3O_4 core–satellite structures, to fabricate nanocomposites based on the thermoplastic polymer PVDF with uniform distribution of these structures in the polymer matrix, and to investigate the structure and dielectric properties of the obtained nanocomposites.

2. Experimental methodology

2.1. Synthesis of $BaTiO_3$-Fe_3O_4 core–satellite structures

0.002 g of polyvinylpyrrolidone was first dissolved in 50 mL of distilled water. Subsequently, 1 g of $BaTiO_3$ was introduced into the solution, and the mixture was stirred at 70°C for 1 h. In the next step, $FeCl_3 \cdot 6H_2O$ and $FeSO_4 \cdot 7H_2O$ were added in amounts of 0.008 and 0.015 mol, respectively. Ammonium hydroxide ($NH_3 \cdot H_2O$) was then added until the pH of the reaction medium reached 11–12. After completion of the reaction, the mixture was cooled to room temperature, and the resulting product was washed six times with ethanol and dried under vacuum at 45°C. This procedure yielded $BaTiO_3$ particles whose surfaces were decorated with Fe_3O_4 nanoparticles.

2.2. Preparation PVDF- $BaTiO_3$-Fe_3O_4 nanocomposites

For the preparation of nanocomposite films, the synthesized $BaTiO_3$–Fe_3O_4 particles were introduced into a thermoplastic PVDF matrix. Thin films were fabricated by solution mixing. First, PVDF was completely dissolved in N,N-dimethylformamide, after which the required amount of $BaTiO_3$–Fe_3O_4 particles was added to the solution. The resulting mixture was stirred for 3 h to ensure uniform filler dispersion, then cast into a glass vessel and dried. As a result, homogeneous PVDF-based nanocomposite structures containing the hybrid $BaTiO_3$–Fe_3O_4 filler were obtained.

2.3. Characterization of nanocomposites

2.3.1. X-ray analysis

Rigaku Mini Flex 600 XRD diffractometer (CuKα radiation from Cu X-ray tube, run at 15 mA and 30 kV) was used for X-ray diffraction analysis at ambient temperature. The nanocomposite films were scanned in the 2θ angle range from 100 to 100°.

2.3.2. Transition electron microscopy (SEM) analysis

TEM analysis of nanocomposites was performed on a JEOL JEM-1400 (Japan), mode at a working voltage of 80-120kV.

2.3.3. Dielectric measurement

Dielectric permittivity of the nanocomposites was determined using a broadband immittance analyzer (MNIPI E7-20). Frequency-dependent measurements were conducted in the range of 25 Hz to 1 MHz at room temperature.

3. Experimental results and their discussion

The structure of $BaTiO_3$ nanoparticles coated with Fe_3O_4 nanoparticles on their surface was investigated by the X-ray diffraction method. The table 1. presents various parameters of the diffraction lines corresponding to the observed peaks. Based on the data presented in the table, it can be concluded that the sample contains both a tetragonal $BaTiO_3$ core and a cubic Fe_3O_4 shell, while PVP, being amorphous, does not produce diffraction peaks [12]. In the 56–58° range, the $BaTiO_3$ (211) and Fe_3O_4 (511) reflections overlap.

Table 1. XRD data of $BaTiO_3$–Fe_3O_4 particles

2θ(deg)	**(hkl) index**	**Characteristic phase**
31.53	$BaTiO_3$ (110)/(101)	a tetragonal $BaTiO_3$ core-
35.59	Fe_3O_4 (311)	magnetite
56.12	Fe_3O_4 (511)+$BaTiO_3$ (211) (overlapped)	Both phase
62.73	Fe_3O_4 (440)	Magnetite

Figure 2 presents the variation of dielectric constant (ε) with frequency for PVDF nanocomposites containing $BaTiO_3$–Fe_3O_4 hybrid fillers. In all cases, ε decreases with increasing frequency, which is a characteristic feature of polymer-based dielectric composites. This behavior is generally associated with interfacial polarization effects. At lower frequencies, space charges can migrate and accumulate at the interfaces between phases, resulting in large dielectric constant values. With increasing frequency, the ability of these charges to respond to the alternating field becomes limited, and the contribution of interfacial polarization correspondingly diminishes, causing a reduction in ε.

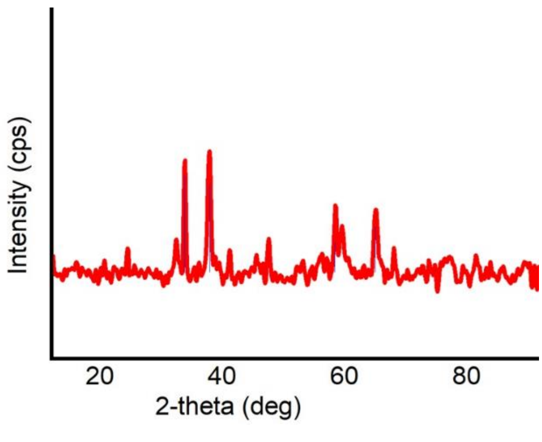

Figure. 1. X-ray diffraction (XRD) patterns of the $BaTiO_3$–Fe_3O_4 particles

The dielectric permittivity of neat PVDF is about 8 at 1 kHz. In contrast, the incorporation of $BaTiO_3$–Fe_3O_4 hybrid nanoparticles leads to a significant increase in dielectric constant at the same frequency. According to Ma et al. (2017), particles with a grain size of 122 nm possess a dielectric permittivity of approximately 2000

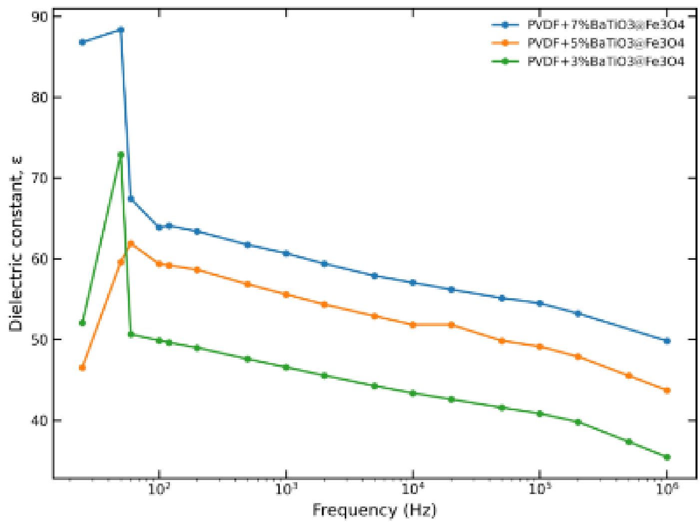

Figure 2. Dielectric constant as a function of frequency for PVDF and $BaTiO_3$–Fe_3O_4- based nanocomposite

at 1 kHz [13]. However, in the present nanocomposites, the measured dielectric constant is considerably lower, and even for the sample filled with 7% $BaTiO_3$–Fe_3O_4, the ε value remains below 60. Such a difference may be related to the magnetite coating on the surface of $BaTiO_3$ particles, which can alter their dielectric contribution, as well as to the relatively low amount of hybrid filler dispersed in the PVDF matrix. Despite this, the increase in dielectric permittivity from about 7–8 for neat PVDF to values approaching 60 clearly demonstrates that the hybrid filler effectively enhances the overall polarization of the system.

Conclusion

In conclusion, novel core–satellite structures consisting of $BaTiO_3$ particles decorated with Fe_3O_4 nanoparticles on their surface were successfully synthesized, and on this basis PVDF-matrix nanocomposites were prepared. The X-ray diffraction results confirm the successful formation of $BaTiO_3$–Fe_3O_4 hybrid nanoparticles composed of a tetragonal $BaTiO_3$ core and a cubic Fe_3O_4 shell, while the absence of diffraction peaks from PVP is consistent with its amorphous nature. This structural organization plays a key role in determining the dielectric behavior of the PVDF-based nanocomposites. The incorporation of these hybrid fillers leads to a pronounced increase in dielectric constant compared with neat PVDF, confirming that the hybrid particles enhance the overall polarization of the system. At the same time, the observed decrease in dielectric constant with increasing frequency indicates that interfacial polarization is the dominant mechanism governing the dielectric response. Although the dielectric permittivity of the nanocomposites remains much lower than that of pure $BaTiO_3$, this can be explained by the Fe_3O_4 coating on the $BaTiO_3$ surface and the relatively low filler content in the PVDF matrix. Nevertheless, the increase in dielectric permittivity from about 8 for neat PVDF to values approaching 60 demonstrates that even a limited amount of $BaTiO_3$–Fe_3O_4 hybrid filler is sufficient to significantly improve the dielectric performance of the polymer matrix.

References

[1] Li C.; Qin H.; Zhou Y.; Yang T.; Chen X.; Li L.; Yuan Z.; Wang K.; Zhang B.; Lu W.; Chen L.; Liu Y.; Bernholc J.; Wang Q. Strain-Induced Polar Interfaces in Ferroelectric Polymer Nanocomposites (Adv. Funct. Mater. 35/2025). *Advanced Functional Materials*. 2025, **35**(35).

[2] Rudravarapu K.; Yarramuthi V.; Munagapati V.S.; Gutha Y.; Wen J.; Prasad C.; Pilla V.a.R.; Gumma L.; Won J.S.; Choi H.Y. Recent progresses in the development of magnetic Fe3O4 nanoparticles supported cellulose-based composites: A review. *Inorganic Chemistry Communications*. 2025, **182**, p. 115588.

[3] Zeng H.; Li J.; Yin H.; Jia R.; Yu L.; Li H.; Xu B. Correction: Zeng et al. Sustainable Synthesis of a Carbon-Supported Magnetite Nanocomposite Anode Material for Lithium-Ion Batteries. Batteries 2024, 10, 357. *Batteries*. 2026, **12**(2), p. 38.

[4] Zaporotskova I.; Muratov D.; Kozhitov L.; Popkova A.; Boroznina N.; Boroznin S.; Vasiliev A.; Tarala V.; Korovin E. Nanocomposites Based on Pyrolyzed Polyacrylonitrile Doped with FeCoCr/C Transition Metal Alloy Nanoparticles: Synthesis, Structure, and Electromagnetic Properties. *Polymers*. 2023, **15**(17), p. 3596.

[5] Li Q.; Ge X.; Ye J.; Li Z.; Su L.; Wu Y.; Yang H.; Song J. Dual ratiometric SERS and photoacoustic Core–Satellite nanoprobe for quantitatively visualizing hydrogen peroxide in inflammation and cancer. *Angewandte Chemie International Edition*. 2020, **60**(13), p. 7323–7332.

[6] Shirinova H.A.; Surkhayli A.E.; Pashayev B.G.; Valimatova N.I. Optimizing thermal behavior in HIPS/silicon nanocomposites: The role of cooling rates. *Journal of Elastomers & Plastics*. 2025, **57**(5), p. 639–655.

[7] Surkhayli A.E.; Pashayev B.G.; Shirinova H.A. Investigation of the kinetic and thermodynamic parameters of polystyrene thermal degradation using dynamic thermogravimetric analysis. *Journal of Physics & Space Sciences*. 2025, **2**(2), p. 31–44.

[8] Hasanli M.R.; Shirinova H.A.; Jafarov M.A.; Pashayev B.G.; Musayeva T.T. Effect of SiO_2 Nanoparticle Concentration on the Mechanical Properties of PS-Based Nanocomposites. *Journal of Physics & Space Sciences*. 2025, **2**(3), p. 78–84.

[9] Huang D.; Yan X.; Yan M.; Zeng G.; Zhou C.; Wan J.; Cheng M.; Xue W. Graphitic Carbon Nitride-Based Heterojunction Photoactive Nanocomposites: Applications and Mechanism Insight. *ACS Applied Materials & Interfaces*. 2018, **10**(25), p. 21035–21055.

[10] Xiang H.; Xing Y.; Dai F.; Wang H.; Su L.; Miao L.; Zhang G.; Wang Y.; Qi X.; Yao L.; Wang

H.; Zhao B.; Li J.; Zhou Y. High-entropy ceramics: Present status, challenges, and a look forward. *Journal of Advanced Ceramics*. 2021, **10**(3), p. 385–441.

[11] Ivanov E.; Kotsilkova R.; Xia H.; Chen Y.; Donato R.K.; Donato K.; Godoy A.P.; Di Maio R.; Silvestre C.; Cimmino S.; Angelov V. PLA/Graphene/MWCNT Composites with Improved Electrical and Thermal Properties Suitable for FDM 3D Printing Applications. *Applied Sciences*. 2019, **9**(6), p. 1209.

[12] Kaliyekperova K.B.; Rusakov V.S.; Kozlovskiy A.L.; Fadeev M.S.; Shlimas D.I.; Zdorovets M.V. Synthesis and investigation of the applicability of Fe3O4/ZnO nanoparticles as a basis for hyperthermic studies. *Case Studies in Chemical and Environmental Engineering*. 2025, **11**, p. 101195.

[13] Ma J.; Chen X.; Ouyang W.; Wang J.; Li H.; Fang J. Microstructure, dielectric, and energy storage properties of BaTiO3 ceramics prepared via cold sintering. *Ceramics International*. 2017, **44**(4), p. 4436–4441.